ELSEVIER

Thermochimica Acta 344 (2000) 95–102

thermochimica acta

www.elsevier.com/locate/tca

Concentration dependence of thermal structural transition of hen egg-white lysozyme under constant heating rate studied by time-resolved SAXS

Mitsuhiro Hirai*, Shigeki Arai, Hiroki Iwase

Department of Physics, Gunma university, 4-2 Aramaki, Maebashi 371-8510, Japan

Accepted 23 August 1999

Abstract

Differential scanning calorimetry (DSC) measurements are well known to serve us heat capacity functions of macromolecules and molar fractions of thermodynamic microstates. On the other hand, small-angle X-ray scattering (SAXS) measurements are expected to have an advantage for determining directly spatial-conformational states of macromolecules since we can observe ensemble-averaged scattering functions from solute macromolecules at multiple spatial-conformational states. In the present paper we will present an approach to analyze spatial-conformational-state transitions observed in denaturation processes of proteins by SAXS, which affords us a new aspect of thermal transition of proteins in comparison with thermodynamic-microstate transitions observed by DSC. From the point of view of spatial-conformational-state transition, we will clarify the thermal structural transition aspects of hen egg-white lysozyme (HEWL) at pH 5 depending on the conformational hierarchy and concentration.

Keywords: Thermal denaturation; Globular protein; Lysozyme; Synchrotron radiation; Small-angle X-ray scattering

1. Introduction

Differential scanning calorimetry (DSC) method is usually used to determine a heat capacity function of macromolecules which afford thermodynamic functions such as calorimetric enthalpy and Gibbs free energy. By using DSC we can also estimate molar fractions of the thermodynamic microstates by using the algorithms for the analysis of DSC curves [1,2]. On the other hand, as an observed scattering function from biological macromolecules in solution reflects an ensemble averaged scattering function of multiple spatial-conformations of solute macromolecules, it can be expected that synchrotron radiation small-angle X-ray scattering (SR-SAXS) measurements have a great advantage for determining directly the spatial-conformational states of macromolecules due to high-intensity beam flux.

We have been studying the thermal denaturation of hen egg-white lysozyme (HEWL) by using SR-SAXS and wide-angle neutron scattering methods. In our recent reports [3,4], we characterized the thermal denaturation processes at pH 1.2, 3.9 and 7.0 and showed that the changes of the tertiary and intramolecular structures proceed in different ways, namely that the former change proceeds in a two-state transi-

* Corresponding author. Tel.: +81-272-20-7554; fax: +81-272-20-7551.
E-mail address: hirai@sun.aramaki.gunma-u.ac.jp (M. Hirai).

0040-6031/00/$ – see front matter
PII: S0040-6031(99)00332-9

tion and that the latter change proceeds in a multi-state transition, where we carried out standard analyses of scattering data such as calculation of radii of gyration and distance distribution functions. In the present paper we will present a new method which would enable us to characterize thermal transition hierarchy and to compare directly spatial-conformational-state transitions observed by SAXS with thermodynamic-microstate transitions observed by DSC in denaturation processes of proteins.

2. Experimental

2.1. Sample preparation and time-resolved SAXS measurements

Hen egg-white lysozyme purchased from Sigma Chemical was solubilized in water solvent at pH 5 adjusted by adding HCl. The protein concentrations of the samples served for SAXS experiments were 1.0%, 2.5% and 5.0% w/v. SAXS experiments were carried out with a SAXS spectrometer installed at the 2.5 GeV storage ring in the Photon Factory, Tsukuba, Japan [5]. The wavelength used was 1.49 Å, and the sample-to-detector distance was 85 cm. A sample cell contained the sample solution was place in a cell-holder whose temperature was controlled by a low-temperature thermostat RC6CP from LAUDA, The temperature of the samples was elevated from 10°C to 84°C at the constant heating rate of 1°C/min, which was monitored by a thermocouple device whose output was recorded by a personal computer through a signal interface. By using a computer-controlled data acquisition system of the SAXS spectrometer, time-resolved SAXS measurements were executed every 1 min with the one-shot exposure time of 55 s.

2.2. SAXS data analyses

As described in detail [3], the following standard data analyses were carried out to experimental scattering curves $I(q)$ after correction of background. The distance distribution function $p(r)$ was obtained by the Fourier transform of the scattering intensity $I(q)$ as:

$$p(r) = \frac{2}{\pi}\int_0^\infty rqI(q)\sin(rq)\mathrm{d}q, \tag{1}$$

where q is the magnitude of scattering vector defined by $q = (4\pi/\lambda)\sin(\theta/2)$ (q is the scattering angle, λ the wavelength). $D_{\max}$ is estimated from the $p(r)$ function satisfying the condition $p(r) = 0$ for $r > D_{\max}$. To estimate radius of gyration R_g of solute particles, we have employed two different methods, namely, the Guinier's method using $\ln(I(q))$ vs. q^2 plot for the small-angle data sets and the Glatter's method using $p(r)$ functions as follows:

$$R_g^2 = \frac{\int_0^{D_{\max}} p(r)r^2\mathrm{d}r}{\int_0^{D_{\max}} p(r)\mathrm{d}r}. \tag{2}$$

For the middle scattering angle region which is larger than the particle size ($qR_g \gg 1$) but smaller compared to typical chemical bond distances a ($qa \ll 1$), it is known that the scattering curves depend on the simple power law given by

$$\log I(q) = \text{constant} + b\log q, \tag{3}$$

where b is called the Porod slope [6]. The evaluation of the Porod slope is useful in characterizing and ascertaining the geometric properties of random structures and polymer chains [7,8].

3. Results and discussion

3.1. Concentration dependence of thermal denaturation process

Fig. 1 shows the temperature dependence of SAXS curves $I(q)$ of the HEWL solutions at pH 5, where Fig. 1a–c corresponds to the protein concentrations of 1%, 2.5% and 5% w/v, respectively. The significant decrease of the scattering intensity below $q \approx 0.02$ Å^{-1} results from the cut-off by the beam stopper. The adjustment of pH only by adding HCl is very important since the presence of repulsive interparticle interaction between HEWL molecules prevents further aggregation caused by thermal denaturation. The broad peak around $q = 0.04$–0.08 Å^{-1} shows the presence of interparticle interaction between solute particles under repulsive Coulomb potential, whose sharpness and position depend on the effective surface charge and concentration of the solute particle [9]. Then the shift of the position of the interparticle correlation peak around $q = 0.04$–0.08 Å^{-1} by elevating temperature indicates that the

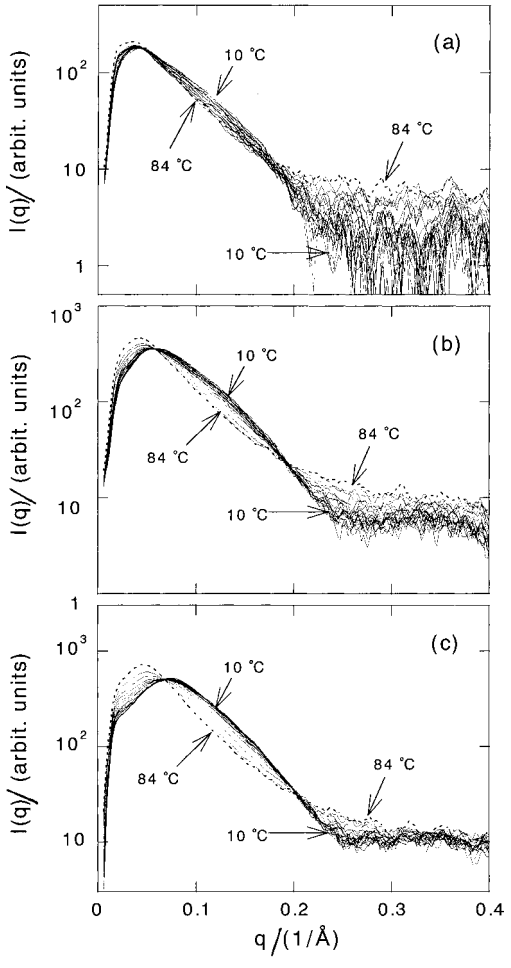

Fig. 1. Time-resolved SAXS curves $I(q)$ of the hen egg-white lysozyme solutions at pH 5 under the constant heating rate of 1°C/min. (a) 1% w/v, (b) 2.5% w/v, (c) 5% w/v. The temperature was elevated from 10°C to 84°C. The scattering curves for every 4 min are presented.

thermal conformational change of HEWL accompanies the change of the molecular surface charge, which is most clearly seen at high concentration in Fig. 1c. For globular particle systems in solution a repulsive interaction between particles usually produces a broad single peak at small q region due to Brownian motion, and the effect of this peak on a scattering curve in the q region above the peak position is negligible [9,10]. The effect of the repulsive interparticle interaction between HEWL molecules on the observed scattering curve is negligible above $q \approx 0.08$ Å^{-1}, which we have shown previously [3]. A scattering curve contains a different real-space structural information of solute particles depending on q range observed. In the present case the change of the scattering curve $I(q)$ in the q range of $\approx$0.1–0.2 Å^{-1} mostly reflects the tertiary structural change in such as molecular shape and dimension, and that in the q range of 0.2–0.4 Å^{-1} mostly reflects the intramolecular structural change in such as structural domain correlation and polypeptide arrangement. Compared with the changing tendencies of the scattering curves in Fig. 1, it is evident that the variation of $I(q)$ in the q range of 0.2–0.4 Å^{-1} with temperature is suppressed by increasing concentration, whereas the variation of $I(q)$ in the q range of 0.1–0.2 Å^{-1} is comparable for every concentration.

Fig. 2a–c shows the temperature dependence of the Porod slope estimated from the scattering curves in

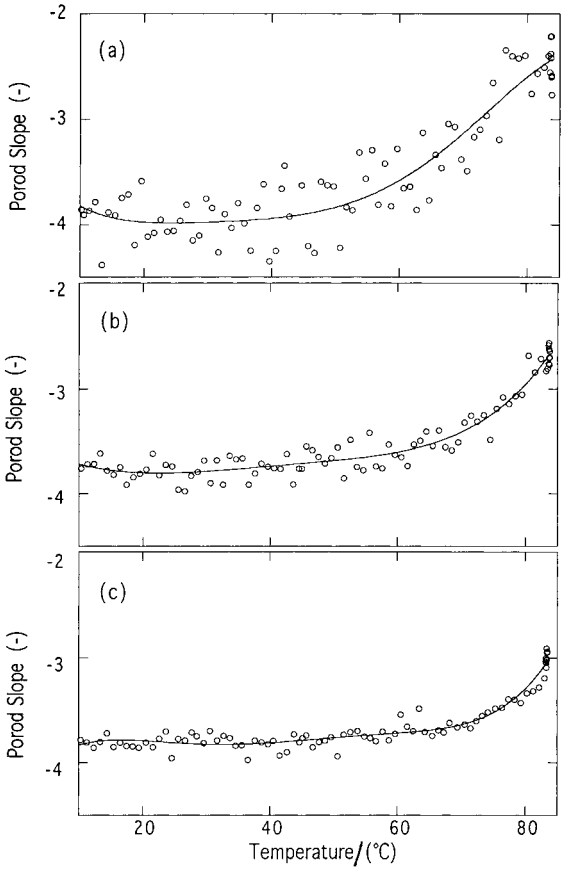

Fig. 2. Temperature dependence of the Porod slopes of the scattering curves in Fig. 1a–c are as in Fig. 1.

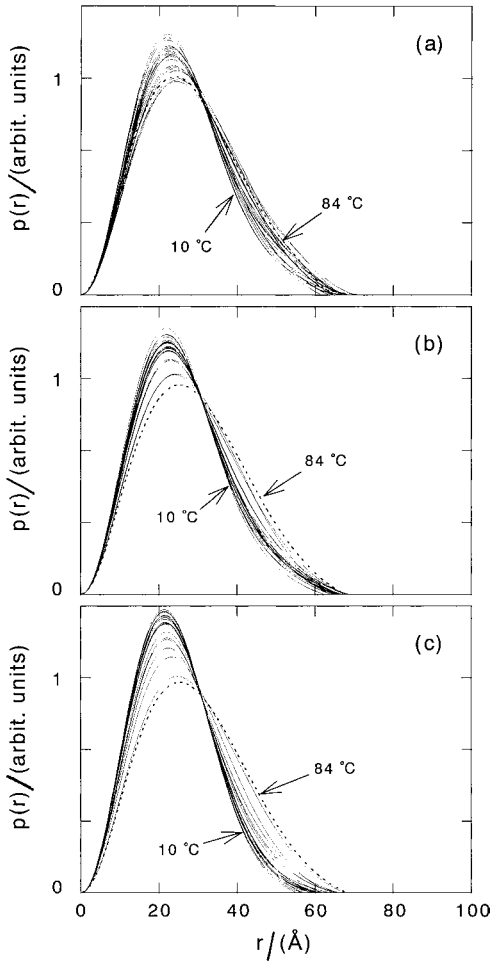

Fig. 3. Distance distribution functions $p(r)$ at different pH depending on temperature. The $p(r)$ functions were obtained by the Fourier transform of the scattering curves in Fig. 1a–c are as in Fig. 1. The $p(r)$ functions for every 4 min are presented.

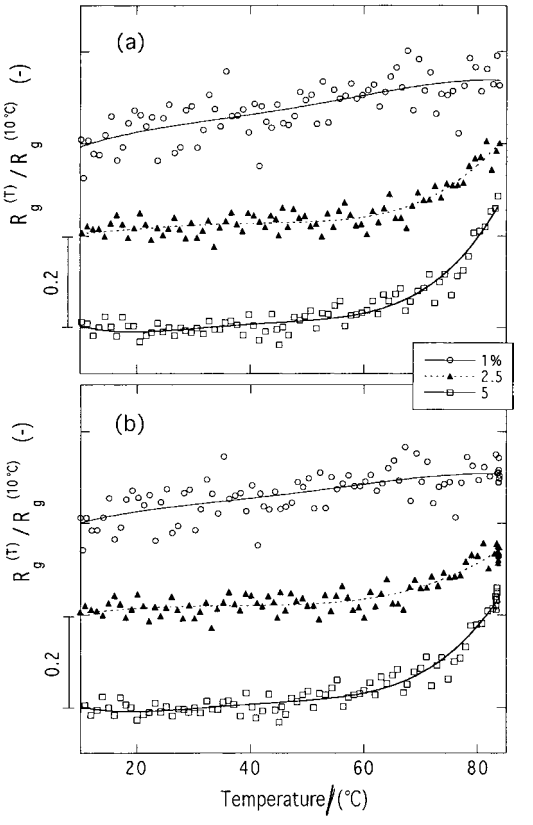

Fig. 4. Temperature dependence of the gyration radii R_g determined by two different methods: (a) by the Guinier's method, (b) the Glatter's method. R_g values are normalized by the R_g values at 10°C. ○, 1% w/v; ▲, 2.5% w/v; □, 5% w/v.

Fig. 1a–c, respectively. With increasing the concentration, the initial temperature of the change of the Porod slope shifts to higher temperature from ca. 50°C to 70°C, indicating that the change of the protein surface from a smooth surface to a fractally rough one [7,8,11,12] is suppressed by increasing the concentration. This agrees with the concentration dependence of the changing tendency of the scattering curve in the q range of 0.2–0.4 $Å^{-1}$ as mentioned in Fig. 1. Fig. 3 shows the distance distribution functions $p(r)$ calculated by the Fourier inversion of the scattering curves in Fig. 1 using Eq. (1). The variation of the $p(r)$ profile depending on temperature well reflects the tertiary structural change. We can recognize an evident concentration dependence of the changing tendency of the $p(r)$ profile. Namely, with decreasing the protein concentration the thermal change of the tertiary structure becomes to proceed rather gradually. This changing tendency is consistent with the temperature dependence of the radius of gyration R_g in Fig. 4, where the relative R_g values obtained by using the Guinier's and Glatter's methods are normalized by the R_g at 10°C values and shown in Fig. 4a and b, respectively. As is well known [13], the use of the Guinier approximation for the determination of R_g is liable to lead to inherent systematic errors and similar difficulties caused by concentration or aggregation

effect. The Glatter's method is more reliable to reduce such artifacts in the estimation of R_g. In Fig. 4 both R_g values estimated by the above two methods give mostly the same temperature and concentration dependence. Thus the changing aspect of R_g with elevating temperature greatly depends on the protein concentration, namely the R_g at 1% w/v increases rather gradually over the observed temperature range, whereas the R_g at 5% w/v increases significantly around ca. 70°C. The remarkable increase of R_g indicates the expansion of the tertiary structural dimension in the thermal denaturation process.

3.2. Temperature differential analysis of scattering curves

To know the margin of the deviation of the scattering curve in the thermal denaturation process of HEWL, we have used the following equation:

$$\frac{\Delta I}{\Delta T} = \frac{\sum_{q=q_1}^{q_2} \left| \frac{\{I(q,T_i) - I(q,T_j)\}}{(T_i - T_j)} \right|}{\left\{ \sum_{q=q_1}^{q_2} I(q,T_i) + \sum_{q=q_1}^{q_2} I(q,T_j) \right\}}, \quad (4)$$

where $\Delta I/\Delta T$ is a normalized temperature differential value of the scattering intensity in the defined q range from q_1 to q_2 in the temperature range from T_j to T_i. Here we set $\Delta T \equiv T_i - T_j = 1$°C. The third term represents the normalization by the integrated intensity in the q range from q_1 to q_2, which is important to compare the deviations of the scattering curve in the different q ranges. Fig. 5 shows the temperature dependence of $\Delta I/\Delta T$ of various q ranges, where Fig. 5a–c corresponds to the $\Delta I/\Delta T$ of the q ranges of 0.1–0.2, 0.2–0.3 and 0.3–0.4 Å^{-1}, respectively. Clearly the temperature differential value $\Delta I/\Delta T$ becomes smaller with increasing protein concentration and that the $\Delta I/\Delta T$ value becomes larger with selecting higher q range used for $\Delta I/\Delta T$ estimation. Thus, Fig. 5 indicates that the increase of the protein concentration reduces the structural fluctuation induced by the temperature elevation, especially the intramolecular structural fluctuation, which supports the discussion in the above section. In comparison with Fig. 5a–c, we can recognize another feature. Thus, the $\Delta I/\Delta T$ of the q range of 0.1–0.2 Å^{-1} tends to increase with elevating temperature and at the high concentration of 5% w/v the $\Delta I/\Delta T$ takes a maximum value around 79°C. This indicates

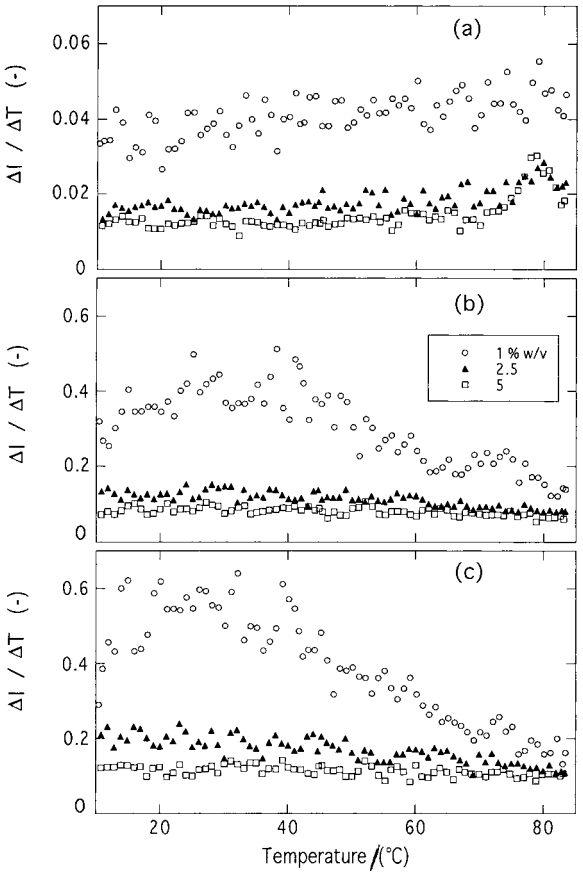

Fig. 5. Normalized temperature differential value $\Delta I/\Delta T$ of the scattering intensity in various q ranges as a function of temperature: (a) 0.1–0.2 Å^{-1}, (b) 0.2–0.3 Å^{-1}, (c) 0.3–0.4 Å^{-1}. The marks of ○, ▲, and □ are as in Fig. 4.

that the significant collapse of the tertiary structure occurs in the relatively narrow temperature region. Whereas, the $\Delta I/\Delta T$ of the q ranges of 0.2–0.3 Å^{-1}. The above aspect suggests that the structural fluctuation induced by the elevation of temperature proceeds in consecutive stages depending on the conformational hierarchy.

3.3. Multiplicity analysis of thermal structural change

To analyze a multiplicity of structural transition by SAXS, we applied the following equation to the scattering curves in a defined q range of q_1–q_2 Å^{-1}

as given by:

$$\Delta = \sum_{q=q_1}^{q_2} \left| \frac{I(q,T)}{\sum_{q=q_1}^{q_2} I(q,T)} - \left\{ \frac{\alpha I(q,T_N)}{\sum_{q=q_1}^{q_2} I(q,T_N)} + \frac{(1-\alpha) I(q,T_U)}{\sum_{q=q_1}^{q_2} I(q,T_U)} \right\} \right|, \quad (5)$$

where $I(q,T_N)$, $I(q,T_U)$ and $I(q,T)$ are the scattering curves at the initial, final and intermediate temperatures, respectively. Under a two-state structural transition hypothesis the factors of α and $(1-\alpha)$ correspond to the molar fractions of the initial and final temperature states when the $I(q,T)$ curve in defined q range is fitted by using the $I(q,T_N)$ and $I(q,T_U)$ curves. Δ represents the deviation factor in the above fitting, namely the deviation from the two-state structural transition hypothesis. The molar fraction α can be determined by minimizing the Δ value. Alternatively, this method using Eq. (5) means that the scattering curve in a defined q region at an intermediate temperature is fitted by using the two scattering curves at the initial and final temperatures since in a defined q region we normalize each scattering curve by the integrated scattering intensity in this q region. Here we assumed that at equilibrium the unfolding transition of HEWL can be described by a population of HEWL proteins with folded (N-state) and unfolded (U-state) stages. This assumption is evidently comparable with the application of the van't Hoff equation to scanning calorimetry analyses for the HEWL samples prepared in the same way used for the scattering experiments, we can also deduce an apparent value of the molar fraction of native state to denatured state from the measured DSC.

Fig. 6 shows the temperature dependence of the α factor at different concentrations, where Fig. 6a–c corresponds to the protein concentrations of 1% and 5% w/v, respectively. In Fig. 6a–c the α factors obtained from the different q ranges of 0.1–0.2, 0.2–0.3 and 0.3–0.4 Å^{-1} are also shown. In the present analysis using Eq. (5) T_N and T_U were 10°C and 84°C. The α factor in the q range of 0.1–0.2 Å^{-1} mostly reflects the change of the molar fraction of the tertiary structures at the initial and final temperatures, while the α factors in the q ranges of 0.2–0.3 and 0.3–0.4 Å^{-1} reflect the change of the molar fraction of the intramolecular structures at the initial and final temperatures. Clearly the changing tendency of the α factor greatly depends both on the q range selected for α estimation and on the protein concentration. The α factor in the q range of 0.1–0.2 Å^{-1}, especially at 5% w/v, changes more significantly in comparison with the cases of the α factor in the q ranges of 0.2–0.3 and 0.3–0.4 Å^{-1}. The above q-range dependence of the changing tendency of the α factor indicates that the thermal structural transition process and its multiplicity greatly depend on the conformational hierarchy. With decreasing the protein concentration the change of the α factor in the q range of 0.1–

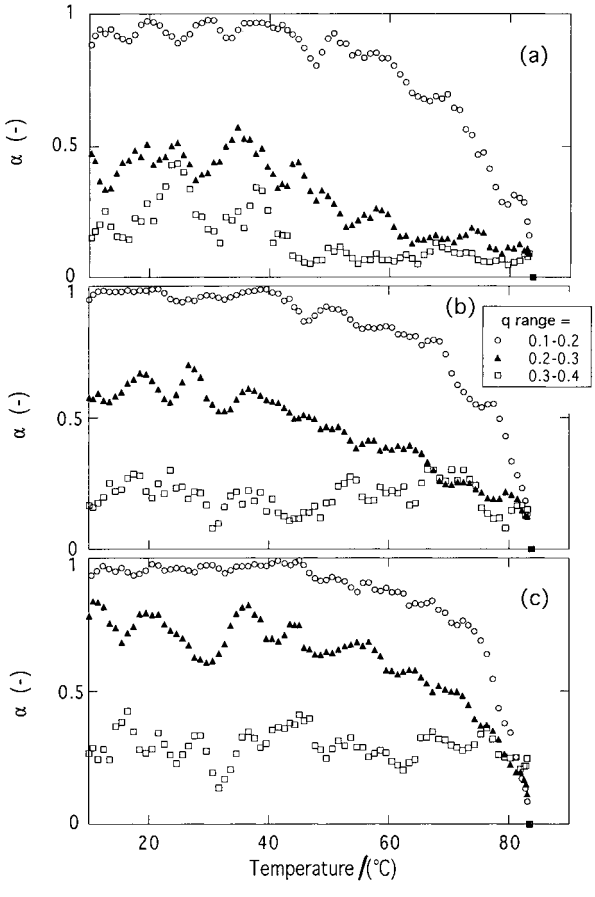

Fig. 6. Temperature dependence of the molar fraction α determined from SAXS data in various q ranges where (a) 1% w/v, (b) 2.5% w/v, (c) 5% w/v. The marks of ○, ▲, and □ correspond to the α factors in q ranges of 0.1–0.2, 0.2–0.3, and 0.3–0.4 Å^{-1}, respectively.

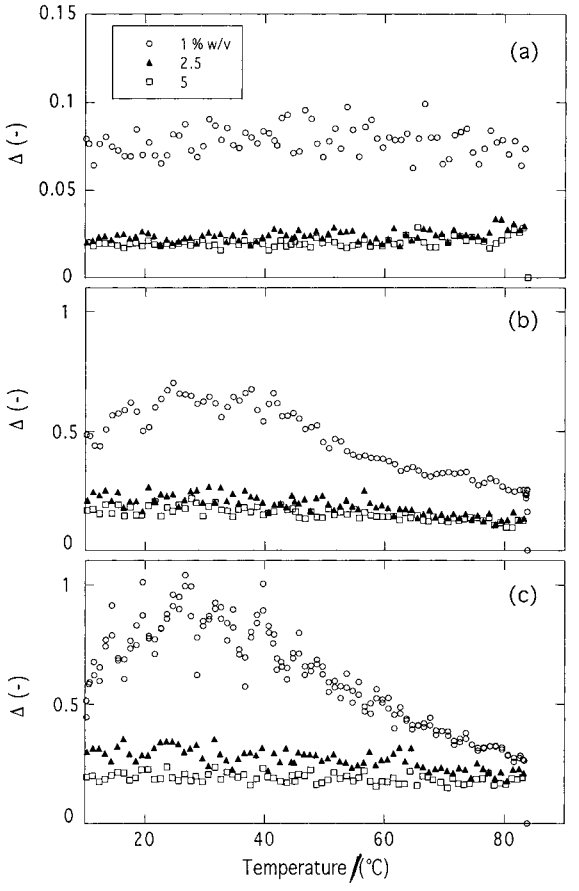

Fig. 7. Temperature dependence of the deviation factors Δ for the optimized values of the molar fraction α in Fig. 6a–c corresponds to the deviation factors Δ obtained from the q ranges of 0.1–0.2 and 0.3–0.4 $Å^{-1}$, respectively. The marks of ○, ▲, and □ are as in Fig. 5.

0.2 $Å^{-1}$ tends to be smeared with shifting the transition midpoint from ca. 79°C to ca. 75°C which was estimated from the temperature at $\alpha \approx 0.5$, suggesting the effect of the protein concentration on the thermal structural transition process.

Fig. 7 shows the temperature dependence of the deviation factor Δ for the optimized α factor in Fig. 6, where Fig. 7a–c corresponds to the Δ factors of the q ranges of 0.1–0.2, 0.2–0.3and 0.3–0.4 $Å^{-1}$, respectively. In Fig. 7a, the Δ factors of the q range of 0.1–0.2 $Å^{-1}$ take very small values and hold mostly constant over the temperature range measured in comparison with those of other q ranges in Fig. 7b and c, suggesting that the α factor analysis based on the two-state transition hypothesis is well applicable to describe the tertiary structural transition kinetics. On the other hand, when we select the higher q range, the Δ factors become lager and larger, indicating that the intramolecular structural transition can not be described by the two-state transition hypothesis but by a multi-state transition. In addition the protein concentration dependence of the deviation factor Δ is clearly recognized, namely, with decreasing the concentration Δ factor becomes to be larger, especially at 1% w/v. This suggests that the multiplicity of the thermal structural transition is enhanced at low concentration.

4. Conclusion

Many studies of thermal denaturation of proteins using DSC have clarified the thermodynamic basis of stability of the conformational states of proteins [14–16], and that at equilibrium unfolding transitions of single domain proteins are usually two-state where only the fully folded and unfolded states are populated [17,18]. Under equilibrium conditions the folding–unfolding transition of HEWL was shown to appear a highly co-operative two-state process [19,20]. On the other hand hydrogen exchange experiments using 2-dimensional NMR show that HEWL consists of the two structural domains which differ significantly in the folding pathway. These structural domains are expected to be stabilized with very different kinetics as distinct folding-domains involving parallel alternative pathways [21–24].

In the present SAXS study we have treated the thermal denaturation of HEWL of the different protein concentrations at pH 5 under a constant heating rate which is comparably used for DSC measurements. By developing new SAXS-data analysis methods we have successfully elucidated other interesting aspects of the thermal structural transition of HEWL depending on the conformational hierarchy and concentration from the point of view of spatial-conformational-state transition. Thus, the temperature differential analysis and the multiplicity analysis suggest that the thermal structural fluctuation depends on the conformational hierarchy of HEWL, namely upon heating the structural fluctuation occurs at first in the polypeptide-chain arrangement and next in the intramolecular

domain correlation, and finally induces the significant collapse of the tertiary structure with such as the change of the radius of gyration and the surface roughness of HEWL. Such a consecutive intramolecular structural fluctuation can not be described by a first-order transition but by a higher-order transition. These above findings well agree with our recent reports [3,4,25]. As mentioned previously [25], a lattice Monte Carlo simulation study of protein folding [26] characterized the folding ability of the polypeptide chain in terms of two intrinsic characteristic temperatures corresponding to transitions of a collapsed structure and a native conformation. This would relate to the present evidences of the thermal structural transition of HEWL characterized in terms of the tertiary and intramolecular structures. With increasing HEWL concentration the above intramolecular fluctuation is suppressed to lead to the abrupt collapse of the tertiary structure at a narrow transition temperature in such a way of two-state transition, suggesting the increase of the protein concentration would stabilize the tertiary and intramolecular structural fluctuations under the presence of strong repulsive intramolecular interaction. In other word at high concentration the presence of the proteins can work as macro ions to stabilize effectively the native conformation, which might be the case for native cells since the concentration of proteins in cells is around 15–18% w/v [27].

Acknowledgements

We thank Prof. Takizawa of Gunma University for his fruitful discussion and Dr. K. Kobayashi of the Photon Factory at the National Laboratory for High Energy Physics for his help with the small-angle scattering instrumentation. This work was performed under the approval of the Photon Factory Program Advisory Committee (Proposal No. 95G094 and 98G186).

References

[1] V.V. V. Filimonov, S.A. Potekhin, S.V. Matveev, P.L. Privalov, J. Mol. Biol. 16 (1982) 435.
[2] S. Kidokoro, H. Uedaira, A. Wada, Biopymers 27 (1988) 271.
[3] M. Hirai, S. Arai, H. Iwase, T. Takizawa, J. Phys. Chem. B. 102 (1998) 1308.
[4] M. Hirai, S. Arai, H. Iwase, T. Takizawa, S. Shimizu, M. Furusaka, Physica B, 241–243 (1998) 1159.
[5] T. Ueki, Y. Hiragi, M. Kataoka, Y. Inoko, Y. Amemiya, Y. Izumi, H. Tagawa, Y. Muroga, Biophys. Chem. 23 (1985) 115.
[6] G. Porod, Kolloid Z. 124 (1951) 251.
[7] T.A. Wittern, L.M. Sander, Phys. Rev. Lett. 47 (1981) 1400.
[8] D.W. Schaefer, K.D. Keefer, Phys. Rev. Lett. 56 (1986) 2199.
[9] M. Hirai, T. Takizawa, S. Yabuki, K. Hayashi, J. Chem. Soc. Faraday Trans. 92 (1996) 4533.
[10] M. Hirai, S. Arai, T. Takizawa, Y. Yabuki, Y. Sano, Phys. Rev. B 55 (1997) 3490.
[11] M. Hirai, T. Hirai, T. Ueki, Macromolecules 27 (1994) 1003.
[12] M. Hirai, R.K. Hirai, S. Yabuki, T. Takizawa, T. Hirai, K. Kobayashi, Y. Amemiya, M. Oya, J. Phys. Chem. 99 (1995) 6652.
[13] L.A. Feigin, D.I. Svergun, in: G.W. Taylor (Ed.), Structure Analysis by Small Angle X-ray and Neutron Scattering, Plenum Press, New York, 1987, p. 68.
[14] P.L. Privalov, N.N. Khechinashvili, J. Mol. Biol. 86 (1974) 665.
[15] C. Tanford, Adv. Protein Chem. 24 (1970) 1.
[16] W. Pfeil, P.L. Privalov, Biophys. Chem. 4 (1976) 23.
[17] P.L. Privalov, S.J. Gill, Adv. Protein Chem. 39 (1988) 191.
[18] P.L. Privalov, Ann. Rev. Biophys. Chem. 18 (1989) 47.
[19] C. Tanford, K.C. Aune, I. Ikai, J. Mol. Biol. 73 (1973) 185.
[20] K. Kuwajima, Proteins: Struct. Funct. Genet. 6 (1989) 87.
[21] A. Miranker, S.E. Radford, M. Karplus, C.M. Dobson, Nature 349 (1991) 633.
[22] S.E. Radford, C.M. Dobson, P.A. Evans, Nature 358 (1992) 302.
[23] S.E. Radford, M. Buch, K.D. Topping, C.M. Dobson, P.A. Evans, Proteins 14 (1992) 237.
[24] M. Buck, S.E. Radford, C.M. Dobson, Biochemistry 32 (1993) 669.
[25] M. Hirai, S. Arai, H. Iwase, J. Phys. Chem. B 103 (1999) 549.
[26] D.K. Klimov, D Thirumalai, Proteins: Struct. Funct. Genet. 26 (1996) 411.
[27] B. Alberts, D. Bray, J. Lewis, M. Raff, K. Roberts, J.D. Watson, in: Molecular Biology of The Cell, Garland Publishing, New York, 1994, p. 90.